Journal of Sound and Vibration (1998) **209**(2), 299–316

INVESTIGATION ON SOUND FIELD MODEL OF PROPELLER AIRCRAFT—THE EFFECT OF VIBRATING FUSELAGE BOUNDARY*

T. Q. WANG AND S. ZHOU

Aeroengine Aerodynamic and Thermal National Laboratory,
Beijing University of Aeronautics and Astronautics, *Beijing* 100083, *Republic of China*

(*Received* 7 *December* 1995, *and in final form* 18 *July* 1997)

The sound field model with multiple propeller noise sources and finite fuselage boundary developed for the prediction of propeller aircraft noise in reference [1] has been improved to take into consideration the effects of vibrating fuselage boundary. The model could be used to solve acoustic–elastic problems, such as calculating the added modal mass and loss factor induced by the interaction between the external sound field and fuselage structure. For demonstration of its application the intermodal coupling coefficients of a scaled fuselage model have been ascertained. For verification purposes the sound field radiated by a sphere with a cyclically vibrating surface has been calculated by this model. The results are coincident with those yielded by an analytical method. The calculation of sound power radiated by a static sphere source gives the model and the numerical method additional proof of their validity. It illustrates that the improved model and its numerical method are valid, reasonable and useful.

1. INTRODUCTION

In reference [1] an improved sound field model of a propeller aircraft with multiple propeller noise sources and finite fuselage boundary has been developed. In it the effects of rigid fuselage boundary on the sound field have been included. In reality, the sound field of the propeller may excite the plate of fuselage to vibrate, and the vibration of the plate may radiate noises. The acoustic–elastic phenomenon of sound field coupling with fuselage structure is the important medium of sound propagating from propeller source into the cabin. It has been confirmed by many measurements in flight tests [2]. In the research of the acoustic–elastic coupling problem, it has been found that the sound pressure on the fuselage is not a blocked pressure, and the sound pressure produced by vibration must be taken into consideration. As illustrated below, the sound field produced by vibration in the transmission of acoustic energy is very important.

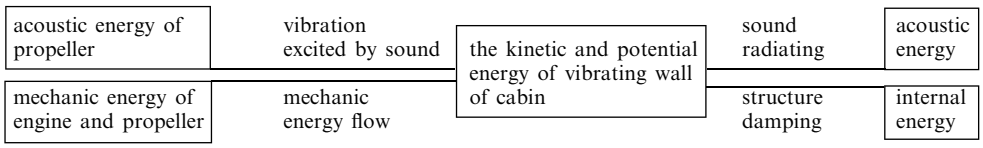

* This work was supported by China Aeronautic Scientific Funding.

0022–460X/98/020299 + 18 $25.00/0/sv971232

In reference [3] the external driving sound field is given by

$$P_T^o(\mathbf{x}') = P_{blT}(\mathbf{x}') + \rho\omega^2 \int G_p^o(\mathbf{x}, \mathbf{x}', \omega) w_T(\mathbf{x})\, d\mathbf{x} \tag{1}$$

where $\mathbf{x}'$, $\mathbf{x}$ represent points of observer and source; $P_{blT}(\mathbf{x}')$ is the transform of the blocked pressure; $G_p^o(\mathbf{x}, \mathbf{x}', \omega)$ is Green's function for the exterior field (source point on the structure); the integral represents the radiated pressure field by the vibrating surface; $w_T(\mathbf{x})$ is displacement of the structure surface; and ω is the angle frequency. In calculating external sound pressure by using (1) it is difficult to find a Green's function satisfying the boundary condition, even though for the most simple problem, such as a cylinder, determining Green's function is also very complicated. It is more difficult to find Green's function for the boundary with an arbitrary shape. Besides that, normally Green's function does not involve the effects of flying speed that introduces a convection effect.

The sound field model with finite fuselage boundary and multi-propeller sources is extended to take into account the effects of the vibrating fuselage boundary with an arbitrary shape. This model can be used to solve the acoustic–elastic problem of the fuselage. An approach to find Green's function in the second item of (1) and to calculate the mass and damping induced by the interaction of external sound field and fuselage structure is presented. The model could also be used to calculate the sound field radiated by any vibrating surface; it has indeed been used to calculate the sound field of static and moving spheres, the surface of which vibrate. The results of a static sphere with an axisymmetrically vibrating surface and a moving compact pulsating sphere are in satisfactory agreement with those yielded by the classical analytical solution and the formulation by Dolling in 1975. This is a good check for the model and the numerical method. The added mass and loss factor for a scaled fuselage model have been calculated. The results illustrate that the present model is reasonable and useful.

2. DESCRIPTION OF THE PROBLEM AND DEVELOPMENT OF THE MODEL

The rigid fuselage boundary condition in reference [1] is modified to take into account the fuselage surface vibrating around the mean surface at small amplitudes. In the frame fixed to undisturbed fluid medium, the co-ordinate $\mathbf{X}$ of a surface point is expressed as

$$\mathbf{X} = \mathbf{X}_0 + \mathbf{n}_m\, w(\mathbf{x}_0, t) \tag{2}$$

where $\mathbf{X}_0$ is the projection co-ordinate of point $\mathbf{X}$ on the mean surface in normal direction; $\mathbf{n}_m$ is the unit normal vector of mean surface; $\mathbf{x}$ and $\mathbf{x}_0$ are the co-ordinates corresponding with $\mathbf{X}$ and $\mathbf{X}_0$ in the frame fixed to the fuselage; and $w(\mathbf{x}_0, t)$ is the normal displacement of surface point from the mean surface at t. Suppose:

$$w(\mathbf{x}_0, t)/L,\ w(\mathbf{x}_0, t)/\lambda \ll 1$$

where L is the characterized length of fuselage, and λ is the wave length. The viscous effects and layer effects are also ignored, keeping the other two hypotheses of reference [1]: (1) The aerodynamic load distribution on a propeller surface and the discrete sound field radiated from this propeller are independent of the presence of fuselage, airfoils and sound field radiated from other propellers (sound is weak pressure perturbation and does not affect the strong fluid field). Hence, it can be calculated separately. (2) The forward velocity of the fuselage is constant, and the Mach number is less then 0·3, so that the refraction effects of boundary layer are small and regligible.

Similar to the rigid fuselage boundary condition, not only the effects of moving propeller

surface but also the fuselage boundary condition can be converted to the sources term on the right side of FW-H equation [4].

$$\frac{1}{c^2}\frac{\partial^2 p}{\partial t^2} - \nabla^2 p = \frac{\partial}{\partial t}[\rho V_n |\nabla f_1| \delta(f_1)] - \frac{\partial}{\partial x_j}[p n_j |\nabla f_1| \delta(f_1)] + \frac{\partial}{\partial t}[\rho V_n |\nabla f_2| \delta(f_2)]$$
$$- \frac{\partial}{\partial x_j}[p n_j |\nabla f_2| \delta(f_2)] + \frac{\partial}{\partial t}[\rho v_n |\nabla f_3| \delta(f_3)] - \frac{\partial}{\partial x_j}[p n_j |\nabla f_3| \delta(f_3)] \quad (3)$$

where $f_1 = 0$ and $f_2 = 0$ represent the equation describing two propellers' surfaces, and $f_3 = 0$ represents the equation describing the fuselage's surface. According to the hypothesis of small vibration amplitude of surface, the sources distributed on the fuselage surface could be approximately replaced by that distributed on the mean surface, which is determined by the normal velocity and pressure on the corresponding position.

$$\frac{1}{c^2}\frac{\partial^2 p}{\partial t^2} - \nabla^2 p = \frac{\partial}{\partial t}[\rho V_n |\nabla f_1| \delta(f_1)] - \frac{\partial}{\partial x_j}[p n_j |\nabla f_1| \delta(f_1)] + \frac{\partial}{\partial t}[\rho V_n |\nabla f_2| \delta(f_2)]$$
$$- \frac{\partial}{\partial x_j}[p n_j |\nabla f_2| \delta(f_2)] + \frac{\partial}{\partial t}[\rho v_n |\nabla f_m| \delta(f_m)] - \frac{\partial}{\partial x_j}[p n_j |\nabla f_m| \delta(f_m)]. \quad (4)$$

The first four terms represent the sources on the propeller surface, while the last two terms represent the sources on the vibrating surface of fuselage. The free field sound pressure of the propeller is generated from the first four terms, and the coupling sound pressure is generated from the last two terms. v_n is the normal velocity of fuselage surface and $f_m(x, t) = 0$ is the equation describing the mean surface.

If the difference between the normal of the moving surface and that of the mean surface is ignored, v_n could be expressed by

$$v_n = V_n + \dot{w}(\mathbf{x}_0, t) \quad (5)$$

where V_n is the normal velocity of mean surface, and $\dot{w}$ is the normal velocity of surface point vibration and is prescribed as assumed. Substituting (5), (4) is reduced to

$$\frac{1}{c^2}\frac{\partial^2 p}{\partial t^2} - \nabla^2 p = \frac{\partial}{\partial t}[\rho V_n |\nabla f_1| \delta(f_1)] - \frac{\partial}{\partial x_j}[p n_j |\nabla f_1| \delta(f_1)] + \frac{\partial}{\partial t}[\rho V_n |\nabla f_2| \delta(f_2)]$$
$$- \frac{\partial}{\partial x_j}[p n_j |\nabla f_2| \delta(f_2)] + \frac{\partial}{\partial t}[\rho V_n |\nabla f_m| \delta(f_m)] - \frac{\partial}{\partial t}[\rho \dot{w} |\nabla f_m| \delta(f_m)]$$
$$- \frac{\partial}{\partial x_j}[p n_j |\nabla f_m| \delta(f_m)] \quad (6)$$

where V_n in the first and third source term is the normal velocity of the propeller surface, and V_n of the fifth term is the normal velocity of the mean surface of the fuselage. According to hypothesis (1), the load on the propeller surface could be obtained from aerodynamic calculation, and is independent of sound field. Therefore the unknown variable in the right side of the equation only exists in the last term. It is the pressure on the fuselage. Because the wave equation is linear, the sound field produced by the fuselage boundary could be divided into two parts. One part is the sound field excited by the propeller's free field sound pressure assuming the mean fuselage boundary is rigid, and the other is the sound field excited by the vibrating fuselage surface in the absence of the external sound field. The latter one is governed by

$$\frac{1}{c^2}\frac{\partial^2 p}{\partial t^2} - \nabla^2 p = \frac{\partial}{\partial t}[\rho \dot{w} |\nabla f_m| \delta(f_m)] + \frac{\partial}{\partial x_j}[p n_j |\nabla f_m| \delta(f_m)]. \quad (7)$$

This indicates that the vibration of the fuselage produces not only a monopole source but also a dipole source which is caused by the coupling pressure distribution. All of these sources could be considered to be distributed on the mean surface.

3. CALCULATING THE SURFACE SOUND PRESSURE EXCITED BY THE VIBRATING FUSELAGE SURFACE

In the Farassat formulation, the pressure excited by the vibrating fuselage is expressed as:

$$4\pi p(\mathbf{x}, t) = \frac{1}{c}\frac{\partial}{\partial t}\int_{f_m=0}\left[\frac{\rho c\dot{w} + p\cos\theta}{r|1 - M_r|}\right]_{ret} \mathrm{d}s + \int_{f_m=0}\left[\frac{p\cos\theta}{r^2|1 - M_r|}\right]_{ret} \mathrm{d}s \tag{8}$$

where the integral surface $f_m = 0$ and retarded equation $g = \tau - t + r/c = 0$ are the same as those used to calculate blocked pressure, $\mathbf{r} = \mathbf{x} - \mathbf{y}$, where $\mathbf{y}$ is the source point on the mean surface $f_m = 0$ at emission time τ. The relations necessary to eliminate the derivative are as follows:

$$\frac{\partial}{\partial t} = \frac{1}{1 - M_r}\frac{\partial}{\partial \tau} \tag{9}$$

$$\frac{\partial r}{\partial \tau} = -V_r \tag{10}$$

$$\frac{\partial M_r}{\partial \tau} = \dot{M}_r + \frac{c}{r}(M_r^2 - M) \tag{11}$$

$$M = V/c. \tag{12}$$

From the above the following is obtained

$$\frac{\partial}{\partial \tau}\left[\frac{1}{r(1 - M_r)}\right] = \frac{r\dot{M}_r + c(M_r - M^2)}{r^2(1 - M_r)^2} \tag{13}$$

$$\frac{\partial}{\partial \tau}\cos\theta = \frac{\partial}{\partial \tau}\left(\frac{\mathbf{n}_m\,\mathbf{r}}{r}\right) = -\frac{V_n}{r} + \frac{V_r\cos\theta}{r}. \tag{14}$$

Using the above relations (9)–(14), (8) could be reduced to

$$4\pi p(\mathbf{x}, t) = \frac{1}{c}\int_{f_m=0}\left\{\frac{(\rho c\dot{w} + p\cos\theta)\,[r\dot{M}_r + c(M_r - M^2)]}{r^2(1 - M_R)^3}\right\}_{ret} \mathrm{d}s$$

$$+ \frac{1}{c}\int_{f_m=0}\left[\frac{p(c\cos\theta - v_n)}{r^2(1 - M_r)^2}\right]_{ret} \mathrm{d}s + \frac{1}{c}\int_{f_m=0}\left[\frac{\rho c\ddot{w} + \dot{p}\cos\theta}{r|1 - M_r|^2}\right]_{ret} \mathrm{d}s. \tag{15}$$

Because of hypothesis (2), $\dot{M}_r = 0$, and regrouping these terms into those that do or do not become singular on the surface, equation (15) becomes

$$4\pi p(\mathbf{x}, t) = \int K_s(\mathbf{x}, t, \mathbf{y}, \tau)\,\mathrm{d}s + \int_{f_m=0} K_R(\mathbf{x}, t, \mathbf{y}, \tau)\,\mathrm{d}s \tag{16}$$

where

$$K_R = \left\{ \frac{\rho c \ddot{w} + \dot{p} \cos\theta}{cr(1 - M_r)^3} \right\}_{ret} \tag{17}$$

$$K_s = \left\{ \frac{\rho c \dot{w}(M_r - M^2) + p[(1 - M^2)\cos\theta - (1 - M_r)M_n]}{r^2(1 - M_r)^3} \right\}_{ret}. \tag{18}$$

If the vibration of the fuselage surface is prescribed and the pressure on the fuselage surface is known, the sound pressure radiated by the vibrating fuselage surface at any observer's point could be calculated by using the above formulation. If the observer's point moves onto the fuselage surface, the equation becomes a singular integral equation. By using the same procedure as that used in the situation of rigid fuselage in reference [1] to remove the singularity of the integral equation [5], the following is obtained:

$$4\pi\left(1 - \frac{1}{2\beta_n^2}\right) p(\mathbf{x}, t) = \int_{f_m = 0} k_s \, \mathrm{d}s + \int_{f_m = 0} k_R \, \mathrm{d}s + \frac{2\pi\rho V_n \dot{w}}{\beta^2} + O(\varepsilon) \tag{19}$$

where the symbols are the same as those used in the calculation of blocked pressure in reference [1]. It is a governing equation to calculate the sound pressure produced by a vibrating surface in the time domain. In this integral differential equation, except the pressure on the fuselage and displacement of the surface, other variables are independent of time. If $\ddot{w}$, $\dot{w}$ have been prescribed, the $p(x, t)$ could be calculated. By using the Fourier transformation, the variable t could be removed, and the governing equation is:

$$4\pi\left(1 - \frac{1}{2\beta_n^2}\right) C_n = \int_{f_m = 0} \left\{ \frac{\mathrm{e}^{-in\omega r/c}[\rho c \mathbf{A}_n (M_r - M^2) + C_n ((1 - M^2)\cos\theta - (1 - M_r)M_n)]}{r^2(1 - M_r)^3} \right\}_{ret} \mathrm{d}s$$

$$+ \int_{f_m = 0} \left\{ \frac{\mathrm{e}^{-in\omega r/c} in\omega[\rho c \mathbf{A}_n + C_n \cos\theta]}{cr(1 - M_r)^3} \right\}_{ret} \mathrm{d}s + \frac{2\pi\rho V_n \mathbf{A}_n}{\beta^2}. \tag{20}$$

C_n and $\mathbf{A}_n$ are the nth Fourier components of surface sound pressure and normal velocity; they are complex functions of the co-ordinate. In the above equation the expression containing C_n is the same as that of equation (8) used to calculate blocked pressure in reference [1], but the expression of sound pressure generated by the nth component of surface vibrating velocity replaces the nth component of free field pressure. It is the equation governing the pressure produced by the fuselage surface, which vibrates in the way prescribed by equation (2).

After discretization a matrix equation is obtained.

$$B(n, \omega, M, f_m) C_n = B_v (n\omega, M, f_m) \mathbf{A}_n \tag{21}$$

where $B(n\omega, M, f_m) = \{B_{ij} (n\omega, M, f_m)\}$ is a coupling matrix, the same as that used in reference [1] for the calculation of blocked pressure; $B_v (n, \omega, M, f_m)$ is a coupling matrix induced by the surface vibration; $\mathbf{A}_n$ is a vector of nth harmonic normal velocity distributed on the fuselage surface; and C_n is the sound pressure distribution on the fuselage surface

induced by the vibration. Both $\mathbf{A}_n$ and C_n are complex numbers which include not only amplitude but also phase. The B_{vij} is as follows:

$$B_{vij} = \left[\frac{e^{-in\omega r_{ij}/c}\rho c(M_{rij} - M^2)}{r_{ij}^2(1 - M_{rij})^3}\right]_{ret}(1 - \delta_{ij})\Delta S_j + \left[\frac{\rho\, e^{-in\omega r_{ij}/c} in\omega}{r_{ij}(1 - M_{rij})^3}\right]_{ret}\Delta S_j + \frac{2\pi\rho V_{ni}}{\beta_i^2}\delta_{ij}. \quad (22)$$

The subscript i represents the observer's point, the subscript j represents the source's point, $n\omega$ is the angle frequency of the harmonic component, and ΔS_j is the element area.

From the above equation the surface sound pressure induced by a vibrating surface, C_n, could be calculated.

$$C_n = B^{-}(n, \omega, M, f_m)B_v(n, \omega, M, f_m)\mathbf{A}_n \quad (23)$$

where $B^{-}(n, \omega, M, f_m)$ is the invert matrix of $B(n, \omega, M, f_m)$.

Now the difficulty mentioned at the beginning of the paper, the calculation of the second term in (1) and Green's functions, have been solved.

The complex sound intensity radiated by the vibrating surface in the normal direction is as follows:

$$I_n = \tfrac{1}{2} P_n * \mathbf{A}_n^*. \quad (24)$$

The real part of the I_n is the active intensity, representing the net sound energy flow radiated or absorbed by the surface. It is produced by the sound pressure and vibrating velocity component that is in phase or 180° out of phase. The image part is the reactive intensity, representing the sound energy circulation. It is produced by the sound pressure and vibrating velocity component that is 90° out of phase.

4. CALCULATION OF THE SOUND FIELD RADIATED BY THE VIBRATING FUSELAGE

If the coupling pressure on the surface of the vibrating fuselage is calculated, the dipole sources generated from pressure distribution on the surface are also determined. From equations (16)–(18) the pressure radiated by the vibrating fuselage surface, in any observer's point out of the fuselage, could be calculated. It is the formulation in the time domain. It can also be converted to the formulation in the frequency domain.

$$4\pi C_n' = \int_{f_m=0}\left\{\frac{e^{-in\omega r/c}[\rho c\mathbf{A}_n(M_r - M^2) + C_n((1 - M^2)\cos\theta - (1 - M_r)M_n)]}{r^2(1 - M_r)^3}\right\}_{ret} ds$$

$$+ \int_{f_m=0}\left[\frac{e^{-in\omega r/c} in\omega(\rho c\mathbf{A}_n + C_n\cos\theta)}{cr(1 - M_r)^3}\right]_{ret} ds \quad (25)$$

where $\mathbf{A}_n$ is the nth component of normal vibration velocity on the surface, and C_n is the nth component of coupling pressure produced by vibration on the surface. In equation (25) the terms containing C_n are the same as the terms containing blocked pressure to calculate scatter pressure of rigid fuselage in equation (12) of reference [1]. It could be said that the dipole sources distribution on the boundary surface generated from coupling pressure of the vibrating surface are the same as that generated from the coupling pressure of the external sound field.

5. COUPLING BETWEEN THE EXTERNAL SOUND FIELD AND THE ELASTIC FUSELAGE STRUCTURE

In the above two sections the surface vibrating velocity is assumed to be known. In transmitting the propeller's noises into an aircraft cabin the fuselage surface vibration is dictated by the coupling of the external and internal sound fields with the elastic fuselage structure, and it could be analyzed clearly in reference [3]. The fuselage structure vibration could be decomposed into a set of structure vibration modes, every one of which has its own eigen-frequency and modal shape. The normal displacement of fuselage structure $w_T(\mathbf{x})$ is expressed as:

$$w_T(\mathbf{x}) = \sum_r \psi^r(\mathbf{x})\xi_{rT} \tag{26}$$

where $\psi^r(\mathbf{x})$ is the rth modal shape of the transmitting structure, and ξ_{rT} is its modal response, i.e., its modal displacement.

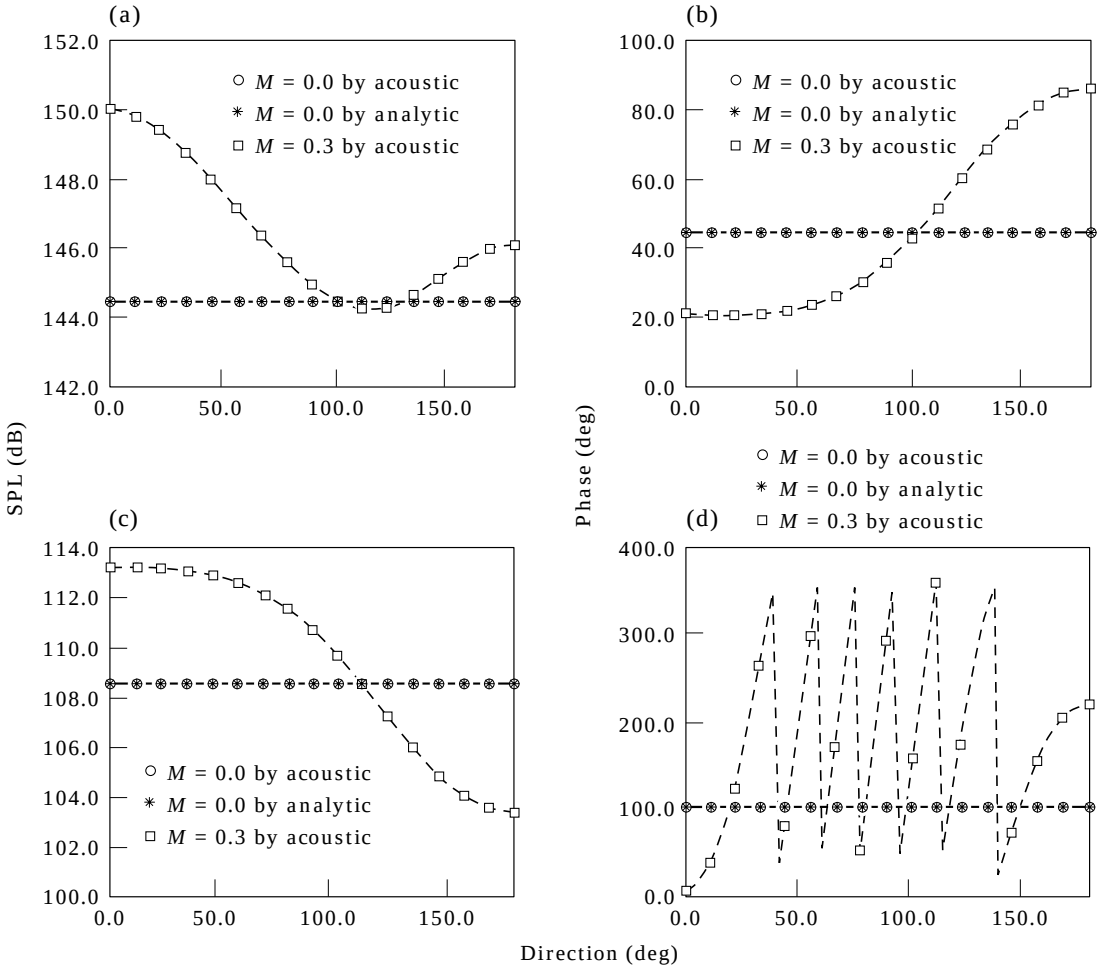

Figure 1. Case 1, $v(\theta) = 0{\cdot}01a\omega$. Comparison of the results for the static sphere obtained by two approaches and the results for the moving sphere calculated by acoustic analogy. (a) Surface SPL; (b) surface SP phase; (c) SPL at $r = 10\lambda$; (d) SP phase at $r = 10\lambda$.

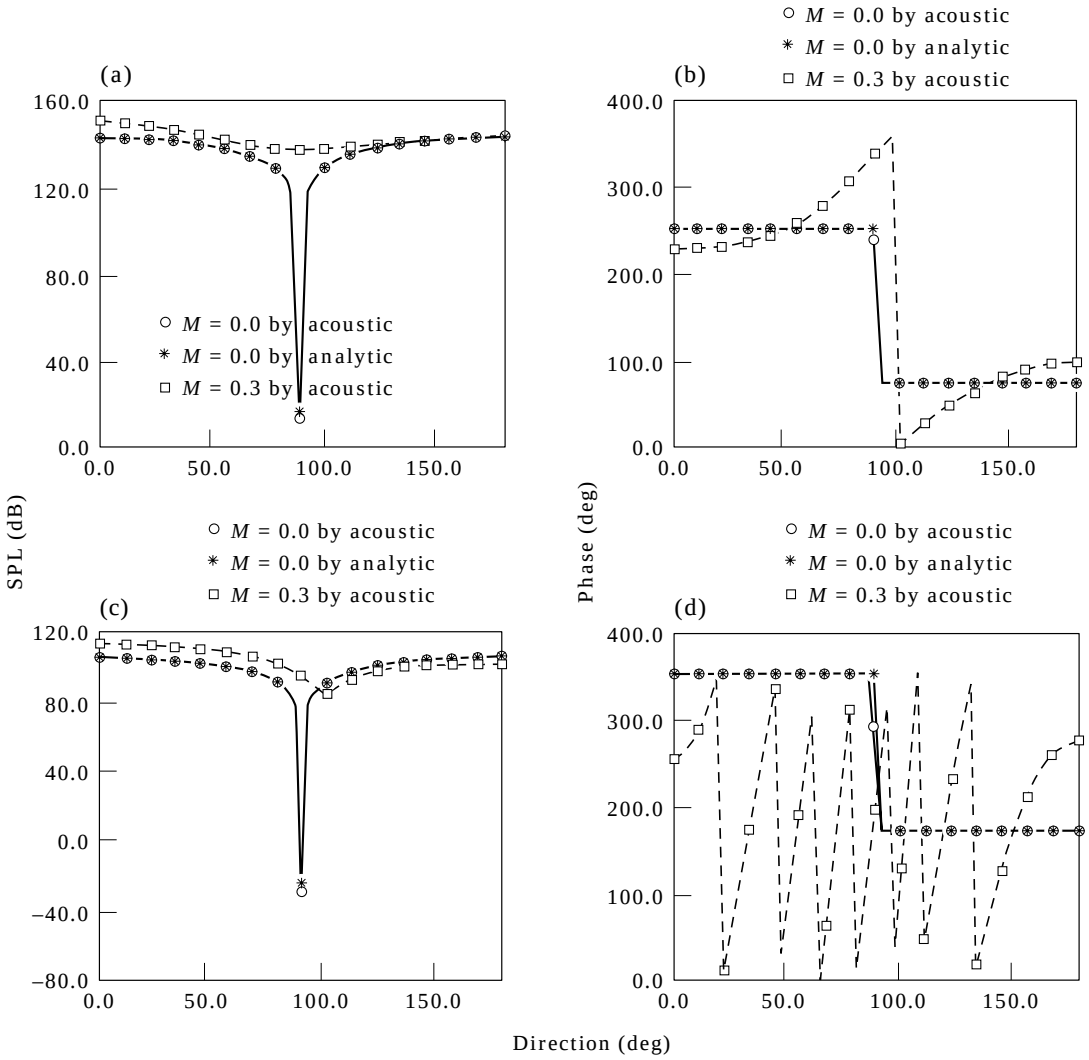

Figure 2. Case 2, $v(\theta) = 0{\cdot}01a\omega \cos(\theta)$. Comparison of the results for the static sphere obtained by two approaches and the results for the moving sphere calculated by acoustic analogy. (a) Surface SPL; (b) surface SP phase; (c) SPL at $r = 10\lambda$; (d) SP phase at $r = 10\lambda$.

In transmitting sound into the cabin, the external acoustical coupling of structure modes is described by the intermodal coupling coefficients defined as:

$$J^{rs}(\omega) = \int\int G_p^o(\mathbf{x}/\mathbf{x}, \omega)\psi^r(\mathbf{x})\psi^s(\mathbf{x}')\,\mathrm{d}\mathbf{x}'\,\mathrm{d}\mathbf{x}. \tag{27}$$

This is a chain element in the chains of sound transmission calculation. The $\rho\omega^2 J^{rs}$ represents the work produced by the surface pressure excited by unit modal displacement of the sth mode, which vibrates at a frequency of ω, in unit modal displacement of the rth mode. The image part of the work is the sound energy which circulates near the surface, and the real part is the net sound energy radiated by the surface. The intermodal mass

M^{rs} and intermodal loss factor η^{rs} induced by the external acoustical coupling of structure modes are defined as:

$$M^{rs} = \rho Im(J^{rs})$$

$$\eta^{rs} = \rho\omega_r/\omega/M^{(r)}Re(J^{rs}) \tag{28}$$

where ω is the angle frequency of the external sound field, ω_r is the response frequency of the rth mode of the fuselage structure, and $M^{(r)}$ is the total modal mass of the rth mode of the structure. The unit of both $M^{(r)}$ and M^{rs} are kg, and the η^{rs} are non-dimensional parameters. While $r = s$, J^{rs} is named automodal coupling coefficients, the M^{rs} and η^{rs} are named as automodal masses and automodal loss factors induced by exterior acoustic coupling of the rth mode of structure.

From equation (23) the expression of $\rho\omega^2 J^{rs}(\omega)$ in discretion form is derived.

$$\rho J^{rs}(\omega) = in\omega\{\psi^r(\mathbf{x}_j\, \Delta S_j\}^T B^-(n, \omega, M, f_m)B_v\,(n, \omega, M, f_m)\{\psi^s(\mathbf{x}_i)\} \tag{29}$$

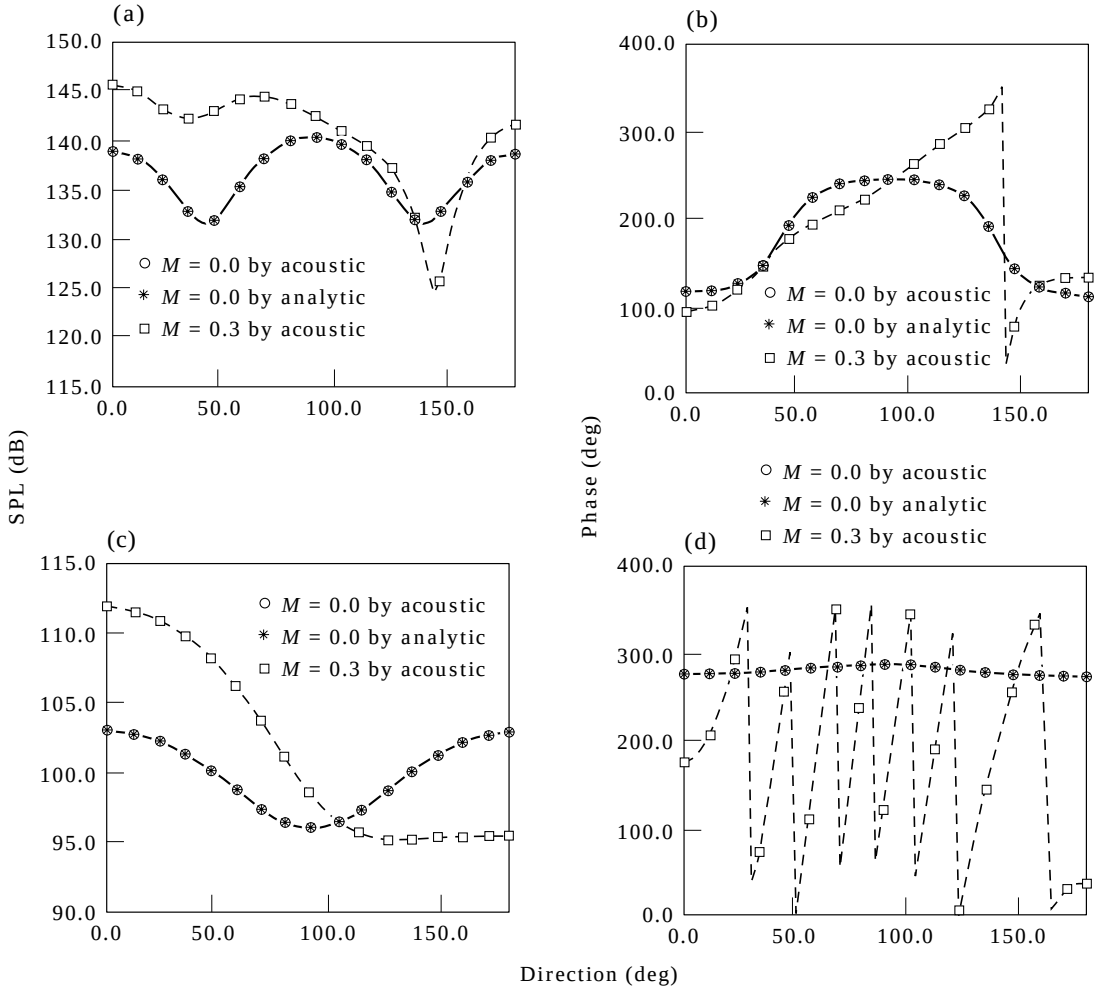

Figure 3. Case 3, $v(\theta) = 0{\cdot}01a\omega\cos(2\theta)$. Comparison of the results for the static sphere obtained by two approaches and the results for the moving sphere calculated by acoustic analogy. (a) Surface SPL; (b) surface SP phase; (c) SPL at $r = 10\lambda$; (d) SP phase at $r = 10\lambda$.

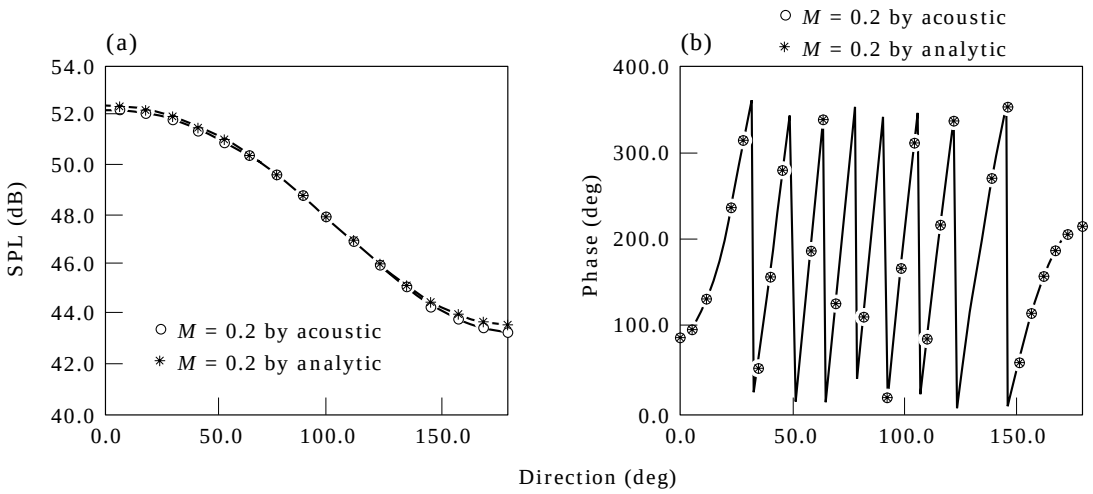

Figure 4. Comparison of SPL normalized (a) and SP phase (b) of a pulsating sphere with a surface intensity of $M = 0{\cdot}2$, at $r = 20\lambda$, by acoustic analogy and analytic expression by dolling.

where $\{\psi^r(\mathbf{x}_j)\Delta S_j\}^T$ is the vector of $\{\psi^r(\mathbf{x}_j)\}$ multiplied by the element area, and the superscript T expresses the operation of rotation of the vector. $n\omega$ is the frequency of the nth harmonic of the propeller.

The coupling coefficients defined in (27) can now be calculated numerically. So far these coefficients have not been calculated, and have been obtained from experiment only.

These coefficients, plus the interior acoustic coupling coefficients, structure modal parameters and generalized blocked force, will determine the modal response of the transmitting structure.

6. CHECK BY THE CASE OF A STATIC SPHERE WITH A VIBRATING SURFACE

The sound field radiated by the axisymmetrically vibrating surface of a sphere could be obtained by the analytical series solution by solving the wave equation [6]. It could be used to check the current approach. Let the radius of the sphere a be 1 m, the wavelength be $2\pi a$, $\rho = 0{\cdot}6678$ kg/m^3, $c = 306$ m/s. The normal velocity shape of the surface vibration is: (1) $V(\theta) = 0{\cdot}01a\omega$—a pulsating sphere with $0{\cdot}01a$ of amplitude; (2) $V(\theta) = 0{\cdot}01a\omega \cos(\theta)$—a rigid sphere vibrating in the axial direction with $0{\cdot}01a$ of amplitude; (3) $V(\theta) = 0{\cdot}01a\omega \cos(2\theta)$—the sphere surface vibrates with $0{\cdot}01a \cos(2\theta)$ of modal shape. For the above three cases, the surface sound pressure and the radiating sound pressure at $r = 10\lambda$ calculated by both analytical series and current approach are in satisfactory coincidence; the difference of SPL is less than 0·1 dB and the difference of phase is less than $0{\cdot}2^\circ$ except for some individual odd points. The results of the three cases are shown in Figures 1–3.

For $\lambda = 2/3\pi a$ and $\lambda = 2/5\pi a$ the same satisfactory coincident results have been obtained.

7. THE SOUND FIELD OF A SPHERE IN MOTION

In the above case, the sphere is stationary. If the sphere is in rectilinear motion, the sound field excited by it will greatly change. The current acoustic analogy approaches are used to calculate the sound fields of a sphere with $M = 0{\cdot}3$ motion velocity and the above

three vibration modes. The results, shown in Figures 1–3, illustrate the big changes of the sound fields. In Figure 1, case 1, it is obvious that both surface pressure and radiating pressure are distributed evenly while the sphere is stationary. But they change by θ while the sphere is in motion. The phase of surface pressure is changed from 21·23° to 86·11°. In the curve of radiating pressure's phase there are six discontinuities where the phase difference between the adjacent points is up to 2π, but there are no discontinuities, if the phase curve is in the Riemann surface.

The results of the other two cases for the sphere when stationary and in motion are similar to the above.

For the sound sources of the uncompacted sphere with moving velocity, there are so far no results available for checking, but more investigations have been made to the compact pulsating sphere sources. Dowling derived an expression of convective amplification of a pulsating sphere in motion at small Mach [7].

$$p = \rho_0 a^2 \dot{v}(\tau_0^*)/(1 - M\cos\theta)^{3\cdot5}/\mathbf{r} \tag{30}$$

where a is the radius of the sphere, $\mathbf{r}$ is the vector distance from source point at the emission time to the observer's point at the reception time, θ is the angle between $\mathbf{r}$ and the direction of movement, and $\dot{v}$ is the normal accelerometer of sphere surface in the emission time. The emission time is approximately calculated by:

$$\tau_0^* = (t - \mathbf{r}/c)/(1 - M\cos\theta). \tag{31}$$

According to the method of convert co-ordinate in reference [8], the expression of sound pressure and the emission time in the reception co-ordinate, which is the co-ordinate in a reference frame that moves with the source, are:

$$p = \rho_0 a^2 \dot{v}(\tau_0^*)/\mathbf{R}[M\cos\Theta + (1 - M^2\sin^2\Theta)^{0\cdot5}]^{2\cdot5}/(1 - M^2\sin^2\Theta)^{1\cdot75}/(1 - M^2)^{2\cdot5} \tag{32}$$

$$\tau_0^* = t - \mathbf{R}[M\cos\Theta + (1 - M^2\sin^2\Theta)^{0\cdot5}]/c/(1 - M^2) \tag{33}$$

where $\mathbf{R}$ is the vector distance from source point to the observer's point in the reception co-ordinate, and Θ is the angle between $\mathbf{R}$ and the direction of movement. These expressions have been used to check the results obtained by the current approach for a compact pulsating sphere at movement of small Mach number.

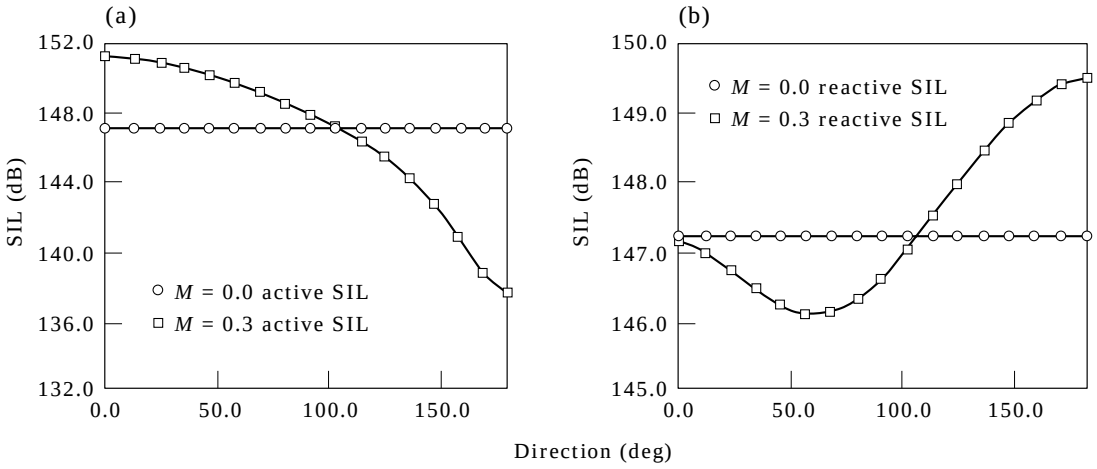

Figure 5. Case 1, surface intensity of $M = 0$ and $M = 0{\cdot}3$. (a) SIL of active intensity; (b) SIL of reactive intensity.

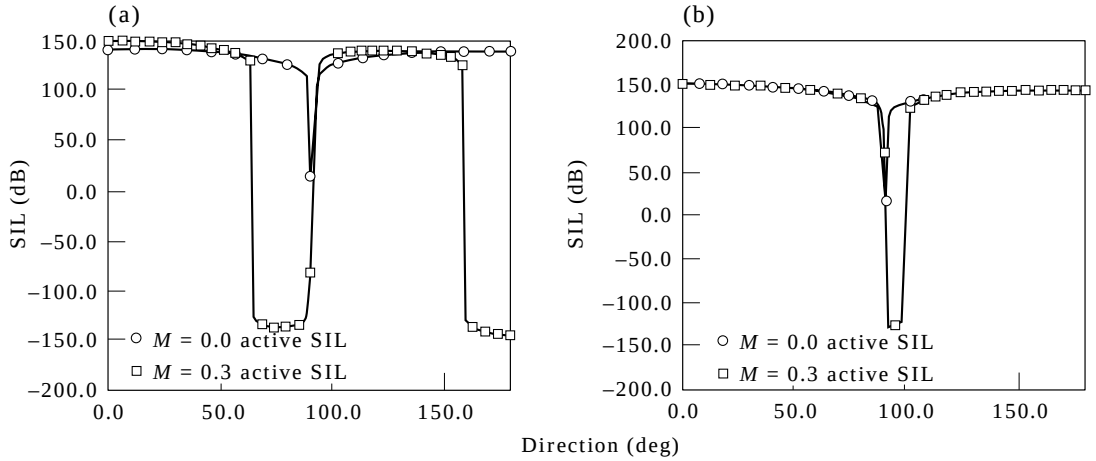

Figure 6. Case 2, surface intensity of $M = 0$ and $M = 0{\cdot}3$. (a) SIL of active intensity; (b) SIL of reactive intensity.

For the pulsating sphere source with $0{\cdot}2M$ and $\lambda = 20\pi a$, the normalized SPL and phase of sound pressure at $r = 20\lambda$ calculated by the two approaches agree very well, as shown in Figure 4.

8. CALCULATION OF THE INTENSITY RADIATED BY SPHERE SOURCES

As for the three normal velocity shapes of a static sphere mentioned in section 6, their surface intensity distribution, including active intensity level and reactive intensity level, are shown in Figures 5–7. The positive value of active intensity means that the surface radiates sound energy, and the negative value means that the surface absorbs the sound energy. The sign of reactive intensity is an indicator of the relative phase of sound pressure and particle velocity.

In case 1, both active and reactive surface intensity have equal positive value due to the surface sound pressure and velocity being distributed evenly and the phase differences

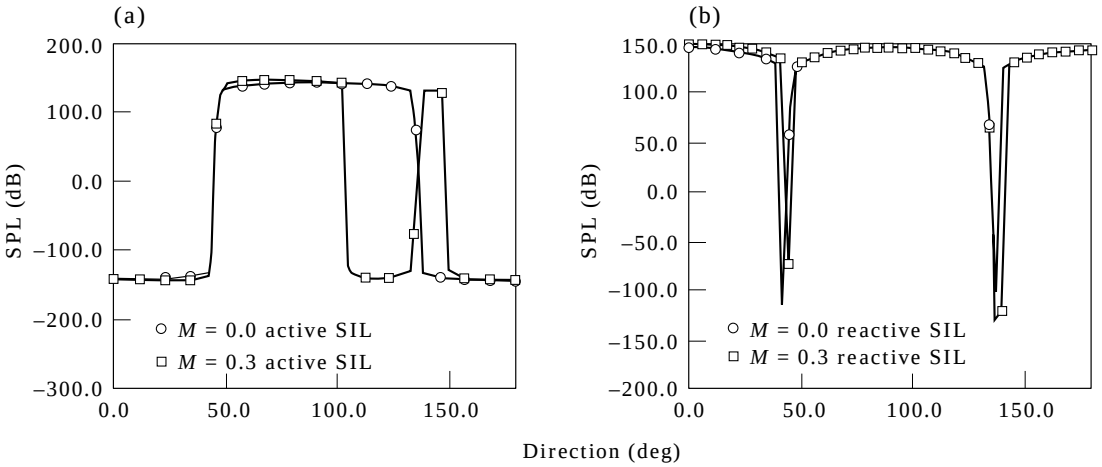

Figure 7. Case 3, surface intensity of $M = 0$ and $M = 0{\cdot}3$. (a) SIL of active intensity; (b) SIL of reactive intensity.

TABLE 1

Sound power level calculated by intensity

	Surface intensity (PWL)	Far field intensity (PWL)
Case 1	158·23	158·23
Case 2	149·46	149·48
Case 3	148·99	148·99

between them being 45°. The distribution of active intensity shows the directivity of monopole. In case 2, the active intensity has positive value, and its distribution shows the directivity of dipole, which is coincident with that of the far field of a vibrating rigid sphere. The reactive intensity has a directivity similar to that of active intensity. In case 3, on the front and rear part of the sphere surface there are negative values of active intensity. Where the active intensity changes direction, the reactive intensity dropped from a positive value to a negative value immediately.

The existence of negative intensity and reactive intensity on the vibrating surface shows that a sound energy circulation is nearby. The surface intensity could be integrated on the surface to get the sound power of the sphere source. In the long distance from the sphere the sound pressure p and particle velocity v are in phase, and $v = p/\rho c$, where the intensity vector points from the center of the sphere to the observer. From the results of the far field sound pressure calculated in section 6, the sound power of sphere source could also be obtained. The values of sound power calculated by the above two approaches are satisfactorily coincident and are listed in Table 1. This is another check for the calculation of the surface sound pressure and the radiating sound pressure of the static sphere.

For the sound field of sphere in motion, $M = 0{\cdot}3$, the surface intensity level is also shown in Figures 5–7, which illustrate the change of sound field caused by the motion. Because the sphere moves, and the intensity direction in the far field is unknown, calculating sound power from the sound pressure in the far field is not applicable.

9. EXAMPLE OF THE COUPLING COEFFICIENCY CALCULATION

For any fuselage structure model, if the mode's shape, describing the normal displacement, and the eigen-frequency could be determined, the intermodal coupling coefficients could be calculated by (29).

Here is an example from Appendix D of reference [9]. It is a ring-stringer stiffened cylinder with a floor partition that is structurally an integral part of the fuselage. The basis of the structural model is an analysis of the free vibrations of a circular cylindrical shell with a longitudinal interior plate (Figure 8) by Peterson and Boyd [10].

The eigenvectors for the fuselage model are the displacements u, v and w for each eigenvalue, ω_r. The w component is the desired mode shape $\psi^r(\mathbf{x})$. This mode shape encompasses both the plate and shell normal displacements. The modes of the shell will couple with the external sound field.

The mode shapes for the symmetric modes of the shell are:

$$\psi_s^r(z, \theta) = \sin\frac{M\pi z}{L} \sum_{n=0}^{n^*} C_{Mn}^{sr} (-1)^n \cos n\theta \tag{34}$$

and for antisymmetric modes

$$\psi_s^r(z, \theta) = -\sin\frac{M\pi z}{L} \sum_{n=0}^{n^*} C_{Mn}^{sr} (-1)^n \sin\theta. \tag{35}$$

In these two equations, z is the axial co-ordinate and θ is measured from the bottom of the cylinder. The C_{Mn}^{sr} are the generalized co-ordinates for the shell.

The symmetric modes of the floor are:

$$\psi_p^r(z, x) = \sin\frac{M\pi z}{L}\sum_{n=0}^{n^*} C_{Mn}^{pr}\cos n\frac{n\pi x}{L_p} \tag{36}$$

and the antisymmetric modes of the floor are

$$\psi_p^r(z, x) = \sin\frac{M\pi z}{L}\sum_{n=0}^{n^*} C_{Mn}^{pr}\sin\frac{n\pi x}{L_p}. \tag{37}$$

Again, z is the axial co-ordinate from the forward end of the cylinder and x is the distance measured horizontally in the floor plate from the centerline of the fuselage to the position of concern on the floor. L_p is the width of the floor.

The modal generalized mass of the fuselage structure includes all energy in both the cylinder and floor and is defined by

$$M^{(r)} = \frac{L}{2}\int_{\theta=0}^{2\pi}(u_s^{r^2} + v_s^{r^2} + w_s^{r^2})m_s\, a\,d\theta + \frac{L}{2}\int_0^{L_p}(u_p^{r^2} + v_p^{r^2} + w_p^{r^2})m_p\,\mathrm{d}x \tag{38}$$

where m_s and m_p are the masses per unit of area of shell and plate respectively, a is the cylinder radius, and L is the cylinder length.

In this example $L = 1{\cdot}803$ m, stiffened $0{\cdot}0008$ m skin, $0{\cdot}508$ m radius with the floor at $56{\cdot}6^\circ$, 32 modes frequency and coefficients of their mode's shape were given in Appendix D of reference [9].

For this scaled fuselage model and a propeller model with 3 blades, of which rotation speed is 4000 r.p.m. and the flying Mach number is $0{\cdot}07$, the intermodal coupling coefficients have been calculated by (29). The added automodal mass and loss factor are tabulated in Table 2 together with the modal mass of the shell structure as well as the modal frequency given by reference [9].

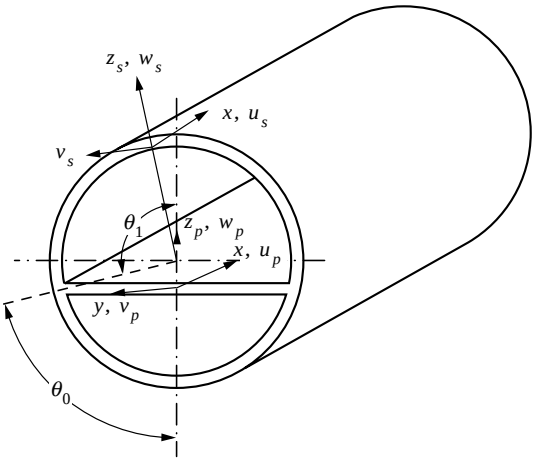

Figure 8. Circular cylindrical shell with a longitudinal partition.

TABLE 2

Added modal mass and loss factor as well as modal mass of structure

Mode r	1	2	3	4	5	6	7	8
Freq (Hz)	188·52	208·24	217·88	231·01	293·25	301·93	303·67	318·73
$M_s^{(r)}$	0·02830	0·05670	0·00143	0·01444	0·0005	2·32876	0·00869	2·87324
M^{rr}	0·00265	0·00426	0·00010	0·00067	0·00002	0·22934	0·00032	0·27738
η^{rr}	0·00187	0·00217	0·00002	0·00003	0·0	0·03110	0·0	0·02588
Mode r	9	10	11	12	13	14	15	16
Freq (Hz)	346·71	434·31	441·78	470·53	502·23	528·78	555·05	558·43
$M_s^{(r)}$	2·38290	0·00025	0·00632	0·82788	2·76903	2·70485	2·55327	0·48102
M^{rr}	0·21613	0·00001	0·00019	0·05975	0·13590	0·15582	0·16752	0·03644
η^{rr}	0·01221	0·0	0·0	0·00065	0·01910	0·00760	0·00341	0·00079
Mode r	17	18	19	20	21	22	23	24
Freq (Hz)	560·65	572·86	591·99	607·50	626·01	632·02	636·15	641·20
$M_s^{(r)}$	0·54454	0·04255	1·52659	1·78872	0·66669	0·51331	0·00018	0·00591
M^{rr}	0·03029	0·00206	0·11540	0·12178	0·03213	0·03093	0·00001	0·00016
η^{rr}	0·00640	0·00002	0·00330	0·00200	0·00009	0·00541	0·0	0·0
Mode r	25	26	27	28	29	30	31	32
Freq (Hz)	648·70	663·30	716·23	717·33	738·44	761·91	779·76	811·04
$M_s^{(r)}$	2·22892	0·00997	0·16827	1·11855	1·85287	2·41279	2·12986	1·69469
M^{rr}	0·16420	0·00626	0·00591	0·10374	0·10110	0·10917	0·11203	0·10048
η^{rr}	0·00350	0·00001	0·00002	0·00368	0·00086	0·00011	0·00021	0·00238

In Table 2, $M_s^{(r)}$ is the modal mass of the shell and the value of added modal masses are much smaller than the modal mass of the structure; the largest one is only a tenth of the modal mass of the shell. The added loss factors are also very small.

The intermodal coupling coefficients ($r \neq s$) are also calculated and most of them are equal to zero, and $J^{rs} = J^{sr}$. A set of typical non-zero values of intermodal masses and loss factors for $r = 6$ are: $M^{6,1} = -0{\cdot}02362$; $M^{6,2} = -0{\cdot}02426$; $M^{6,3} = 0{\cdot}00018$; $M^{6,4} = 0{\cdot}00025$; $M^{6,5} = 0{\cdot}00005$; $M^{6,7} = 0{\cdot}00010$; $M^{6,10} = 0{\cdot}00001$; $M^{6,11} = 0{\cdot}00003$; $M^{6,13} = 0{\cdot}01819$; $M^{6,15} = 0{\cdot}00857$; $M^{6,19} = -0{\cdot}00493$; $M^{6,24} = 0{\cdot}00002$; $M^{6,25} = 0{\cdot}00800$; $M^{6,30} = -0{\cdot}00182$.

The intermodal loss factors are: $\eta^{6,1} = -0{\cdot}00337$; $\eta^{6,2} = -0{\cdot}00382$; $\eta^{6,3} = -0{\cdot}00003$; $\eta^{6,4} = -0{\cdot}00003$; $\eta^{6,5} = -0{\cdot}00002$; $\eta^{6,7} = -0{\cdot}00004$; $\eta^{6,13} = -0{\cdot}00055$; $\eta^{6,15} = -0{\cdot}00721$; $\eta^{6,19} = 0{\cdot}00143$; $\eta^{6,24} = -0{\cdot}00002$; $\eta^{6,25} = -0{\cdot}00119$; $\eta^{6,30} = -0{\cdot}00026$.

Until now the calculation for external acoustic coupling has been finished. In this case the external acoustic coupling effects do not play an important role compared with the modal parameters of structure.

10. CONCLUSION

The acoustic analogy method has successfully been used to develop a discrete sound field model of a propeller aircraft and its numerical calculation method, which account for the effects of the fuselage boundary moving constantly with less than 0·3 Mach number and vibrating with a known vibration shape. Generally both the model and calculation method could solve the problem of the sound field generated by any harmonically vibrating boundary and acoustic–elastic problem.

By using this model the sound field of sphere sound sources has been calculated, and the result is in satisfactory agreement with the analytical result obtained from the serial solution of the static sphere and the formulation by Dolling for the compacted sphere in motion at small Mach numbers. The calculation of sound intensity on the surface of the sphere illustrates the sound energy flow near the sphere, and the sound power calculated gives another check for this approach.

The calculation of the intermodal coupling coefficients opens a way to account for the coupling between the external sound field and elastic fuselage structure. The modal coupling coefficients calculated for a scaled fuselage model gives an example of application.

All of these illustrate the validity of both the model and the calculation method.

REFERENCES

1. T. Q. Wang and S. Zhou 1997 *Journal of Sound and Vibration* **207**. Investigation on sound field model of propeller aircraft—the effects of rigid fuselage boundary.
2. T. Q. Wang and Y. S. Sheng 1992 14*th ICA*. An analysis of the sound transmission path inside the light propeller aircraft using sound intensity measurement.
3. L. D. Pope and J. F. Wilby 1977 *J.A.S.A.* **62**, 906–911. Band-limited power flow into enclosures.
4. J. E. Ffowcs Williams and D. L. Hawkings 1969 *Pil. Trans. Roy. Soc.* **264A**, 321–341. Sound generation by turbulence and surface in arbitrary motion.
5. L. N. Long 1983 *NASA TP* 2197. The compressible aerodynamics of rotating blade based on acoustic formulation.
6. P. M. Morse and K. V. Ingard 1968 *Theoretical Acoustics*. New York: McGraw-Hill.
7. A. Dowling 1976 *J. Fluid Mech.* **74**, 529–546. Convective amplification of real simple sources.
8. A. P. Dowling and J. E. Ffowc Williams 1983 *Sound and Sources of Sound*, Chapter 9. 186–199. Elliss Horwood Limited.

9. L. D. Pope, E. G. Wilby and J. F. Wilby 1984 *NASA CR*-3818 Propeller aircraft interior noise model.
10. M. R. Peterson and D. E. Boyd 1978 *Journal of Sound and Vibration* **60**, 45–62. Free vibration of circular cylinder with longitudinal, interior partitions.

APPENDIX: NOMENCLATURE

$\mathbf{A}_n$	the nth component of normal vibration velocity on surface
a	radius of sphere
$B(n\omega, M, f_m)$	a coupling matrix for rigid boundary
$B_v(n\omega, M, f_m)$	a coupling matrix for vibrating boundary
C_n	nth pressure component on surface
C'_n	nth radiating pressure component
c	sound velocity
f, f_1, f_2	function describing blade surface
f_3, f_m	function describing fuselage surface
G_p^0	exterior field Green's function
$J^{rs}(\omega)$	intermodal coupling coefficients of rth and sth modes
k	wave number
K_R	regular kernel
K_S	singular kernel
l_j	load on surface
$\dot{l}_j$	time derivative of load
$M = V/c$	Mach number
$M_n = V_n/c$	Mach number in normal direction
$M_r = \mathbf{V}\mathbf{r}/c$	Mach number in propagation direction
M_t	Mach number in tangential direction
M^{rs}	added modal mass
if $r = s$	automodal mass
if $r \neq s$	intermodal mass
$M^{(r)}$	modal mass of structure
$\mathbf{n}, \mathbf{n}_m$	unit normal vector of surface
$p(x, t)$	sound pressure
$\mathbf{R}$	vector distance in reception co-ordinate
$\mathbf{r} = \mathbf{x}(t) - \mathbf{y}(\tau)$	vector distance between source and observer
$r = \lvert\mathbf{r}\rvert$	
$\hat{r} = \mathbf{r}/r$	
t	observer time
$\mathbf{V}$	velocity of body
V_n	normal velocity of body
$w(x_0, t)$	normal displacement of surface point from mean surface
$\mathbf{X}$	observer position in frame fixed to undisturbed fluid medium
$\mathbf{X}_0$	the projection co-ordinate of $\mathbf{X}$ on mean surface
$\mathbf{x}$	observer position in frame moving
$\mathbf{x}_0$	the point on mean surface in frame moving
$\mathbf{y}$	source position in frame moving
$\beta = \sqrt{1 - M^2}$	
$\beta_n = \sqrt{1 - M_n^2}$	
$\delta(f)$	Dirac delta function
ε	size of small square hole removed from integral
Θ	the angle between $\mathbf{R}$ and the direction of movement
θ	the angle between $\mathbf{r}$ and $\mathbf{n}$ or $\mathbf{V}$
ρ	density of the undisturbed medium
τ, τ_0^*	retarded time (i.e., time of emission)
ω	angular frequency
ω_r	response frequency of rth mode of the structure
η^{rs}	added loss factor
if $r = s$	automodal loss factor
if $r \neq s$	intermodal loss factor

$\psi^r(\mathbf{x})$	rth modal shape vector of structure
ξ_{rT}	rth modal response of structure

Subscript

ret	expression is evaluated at retarded time

Superscript

$\dot{}$	expression of time derivative
$\fint$	integration with a specific hole removed from region of integration